Particle charge in the bulk of gas discharges

S. A. Khrapak,[1] S. V. Ratynskaia,[1] A. V. Zobnin,[2] A. D. Usachev,[2] V. V. Yaroshenko,[1] M. H. Thoma,[1] M. Kretschmer,[1] H. Höfner,[1] G. E. Morfill,[1] O. F. Petrov,[2] and V. E. Fortov[2]

[1]*Max-Planck-Institut für Extraterrestrische Physik, D-85741 Garching, Germany*

[2]*Institute for High Energy Densities, Russian Academy of Sciences, Izhorskaya 13/19, 125412, Moscow, Russia*

(Received 3 February 2005; revised manuscript received 13 April 2005; published 28 July 2005)

An experimental determination of particle charge in a bulk dc discharge plasma covering a wide range of neutral gas pressures, was recently reported [S. Ratynskaia *et al.*, Phys. Rev. Lett. **93**, 085001 (2004)]. The charges obtained were several times smaller than the predictions of collisionless orbital motion limited theory. This discrepancy was attributed to the effect of ion-neutral collisions. In the present paper a more detailed description of this experiment is provided and additional experimental results obtained with particles of different sizes are reported. The measurements are compared with molecular dynamics simulations of particle charging for conditions similar to those of the experiment, with other available experimental data on particle charge in the bulk of gas discharges, and with a simple analytical model accounting for ion-neutral collisions. All the considered evidence indicates that ion-neutral collisions represent a very important factor, which significantly affects (reduces) the particle charge under typical discharge conditions.

DOI: 10.1103/PhysRevE.72.016406 PACS number(s): 52.27.Lw, 52.20.−j, 52.35.−g

I. INTRODUCTION

Complex (dusty) plasmas consist of ionized gases containing charged particles (grains) of condensed matter. Dust and dusty plasmas are quite natural in space: e.g., in planetary rings, comet tails, and interplanetary and interstellar clouds [1–3]. Dust particles are often present in plasmas used for industrial applications [4,5] and in thermonuclear facilities with magnetic confinement [6,7]. In laboratory conditions, depending on the strength of the interaction between the grains, complex plasmas can exhibit properties of crystals, liquids, and gases. In addition, the overall dynamical time scales associated with the grain component are relatively long and the grains can be easily visualized. The unique feature of observing kinetic properties in real space and time makes it possible to study generic universal processes (e.g., phase transitions, crystallization, transport, wave phenomena, self-organization, and scaling in fluid flows, etc.) in a detail not accessible so far, and at a more fundamental level [8–12]. Not surprisingly, the field of complex (dusty) plasmas has received considerable attention and has shown rapid sustained growth over the last two decades.

The particle charge is one of the most important parameters of complex plasmas. In typical laboratory experiments using gas discharges the (negative) charge on a grain is determined by the balance of electron and ion fluxes to its surface. To calculate these fluxes the orbital motion limited (OML) theory (see, for example, Refs. [13,14]) is usually used. This approach deals with collisionless electron and ion trajectories in the vicinity of a small individual probe (dust particle) and allows the determination of the cross sections for electron and ion collection only from the conservation of energy and angular momentum. However, the assumptions underlying OML theory are seldom met in real dusty plasmas. Let us discuss three major reasons, which can make the OML approach inapplicable.

The first is associated with finite dust density in experiments and is known as the effect of "closely packed" grains. This effect is twofold. The grain component contributes to the quasineutral condition, making the ion density larger than the electron density [15]. This increases the ratio of the ion-to-electron flux and hence reduces the absolute magnitude of the grain charge compared to the case of an individual grain. The strength of the effect can be characterized by the value of the parameter $P=Zn_d/n_e$ (often called the Havnes parameter), where Z is the absolute magnitude of grain charge in units of elementary charges and $n_d(n_e)$ is the grain (electron) density. The charge tends to that of an individual particle when $P \ll 1$, while it is reduced considerably for $P \gg 1$. In addition, when the interparticle separation Δ is smaller than the plasma screening length λ, then the ion and electron trajectories are affected by interactions with neighboring particles, thus influencing grain charging. Barkan *et al.*[16] demonstrated experimentally that the effect of closely packed grains can lead to substantial charge reduction.

The second reason is associated with the fact that OML theory presumes the absence of a barrier in the *effective potential energy* U_{eff} of interaction between the dust grain and plasma particles. The barrier is absent for repulsive interaction (i.e., for the electrons) but can be present for attractive interaction (i.e., for the ions). It can be shown that the barrier is absent only when the electrostatic potential around the grain decays more slowly than $1/r^2$ [17]. In reality, however, the potential scales as propontional to $1/r$ close to the grain, propontional to $1/r^2$ far from it, and at intermediate distances the potential can decrease faster. As a result, a barrier in U_{eff} exists for ions moving toward the grain and some (low energy) ions are reflected from this barrier and cannot reach the grain surface. This effect leads to a decrease in the ion current compared to OML theory and, hence, to an increase in Z. For a Maxwellian ion velocity distribution there are always sufficiently slow ions, which are reflected from the barrier in U_{eff} [18]. However, it can be shown that for a model Debye-Hückel (Yukawa) interaction potential the corrections to the OML model are negligible as long as the grain

radius is considerably smaller than the screening length [12,19,20]. The same conclusion is drawn in Ref. [14] from a consistent solution for the surface potential, electrostatic potential distribution around the grain, and the distribution of ion trajectories.

The third reason is due to collisions. In the OML approach collisions of electrons and ions with neutrals are neglected on the basis that the electron and ion mean free paths $\ell_{e(i)}$ are long compared to the plasma screening length [21]. However, theory has shown that ion-neutral charge-exchange collisions in the vicinity of a small probe or dust grain can lead to a substantial increase in the ion current to their surfaces even when ℓ_i is larger than λ [22–24]. An increase of the ion current to cylindrical Langmuir probe at moderate pressures is also a known effect, which is attributed to ion-neutral collisions [25–28]. The enhancement in the ion current can considerably reduce the grain charge.

The problems in applying OML theory to real complex plasmas show the importance of experimental investigations of particle charging. So far most of the experiments were performed in sheath or striation regions of discharges [29–35]. The comparison with theory is complicated here due to a strong plasma anisotropy, non-neutrality, presence of "suprathermal" ions and electrons, etc. In addition to the charging model one needs to choose an appropriate model for the sheath, which is itself a sophisticated task.

Recently experimental results on grain charges in a bulk dc discharge plasma extending over a wide range of neutral gas pressures were reported by Ratynskaia *et al.*[36]. The charges obtained were several times smaller than predicted by the collisionless OML model, which was attributed to the effect of ion-neutral collisions. In the present paper we provide more details on the experiment, the theoretical models used, and the validity of the approximations employed in Ref. [36]. Additional experimental results obtained with grains of different sizes are presented. A simple analytical approximation of charge dependence on "ion collisionality" proposed by Lampe *et al.* [24] is shown to agree well with the experimental results. The obtained results are also compared with other available measurements of grain charge in a bulk plasma. The results of this analysis clearly demonstrate that under typical experimental conditions in laboratory complex plasmas the particle charge is considerably reduced compared to the prediction of the OML theory.

II. EXPERIMENT

A. Experimental setup

The experiment is performed with the Plasma Kristall-4 (PK-4) facility. This is an experimental project for investigating complex dc and combined dc/rf plasmas under microgravity conditions onboard the international space station (ISS) after 2007 [37]. The PK-4 facility is particularly suited to study phenomena in fluid flows of complex plasmas in the "liquid" state. First experiments have been conducted in the laboratory and in parabolic flight campaigns in a German-Russian collaboration. The experiments described in this paper were done in ground-based conditions.

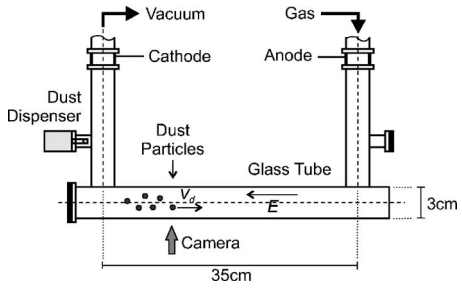

FIG. 1. Sketch of the experimental setup.

A dc discharge is operated in a 35 cm long U-shaped glass tube with a radius of $R=1.5$ cm filled with neon gas at pressures 20–150 Pa and at a current of 1 mA (voltage of $\sim$1–3 kV). The setup is sketched in Fig. 1. The complex plasma is formed by injecting spherical Melamine-formaldehyde particles with mass density of 1.51 g/cm^3 into the discharge. The radii of the particles used in the experiment are $a \simeq 0.6$, $\simeq 1.0$, and $\simeq 1.3$ μm. The injected particles are captured by the plasma and, being charged negatively, drift against the discharge electric field in the horizontal part of the tube (see Fig. 1). For the grain sizes used in our experiments the weak ambipolar radial electric field in the bulk plasma is sufficient to compensate against gravity so that in radial direction the grain cloud is confined to a relatively narrow region near the axis of the tube.

The particle flow is illuminated by a laser sheet with a width of 100 ± 30 μm. The particle motion is recorded by a charge-coupled device video camera with a field of view of 6.4×4.8 mm^2 and rate of 120 frames per second. Each image corresponds to an exposure time of 8 ms. The measurements are taken with the camera positioned as shown in Fig. 1. It was confirmed that the particle dynamics is essentially the same along the tube. The dust number density n_d can be estimated by counting the number of particles in single video images. The grain velocities V_d can be obtained by tracking individual particles through the video sequences or measuring the length of a particle track in a single image. The velocities of the grains exhibit no radial dependence, apparently due to small radial extent of the cloud compared to the radius of the tube.

Probe measurements of plasma parameters are performed in the absence of grains [37]. For the relatively small discharge current used in experiment, care must be taken to minimize probe size in order to avoid significant plasma perturbation and correspondingly, to minimize the size of the probe holder to avoid its influence on the probe measurements [38]. The probe used has a length of 4.5 mm and a radius of 25 μm. The radius of the probe glass holder is decreasing from 0.3 to 0.1 mm near the probe tip. To decrease the effect of plasma potential fluctuations, the measurements of the probe potential were performed with respect to a reference probe of similar dimensions installed in the vicinity of the measuring probe. At the same time the measurements of the probe current were performed using the anode electrode. For the plasma parameters and probe dimensions used in the experiment, the electrons are in the collisionless regime and, thus, the Druyvesteyn formula is used to calculate the electron density n_e and the electron

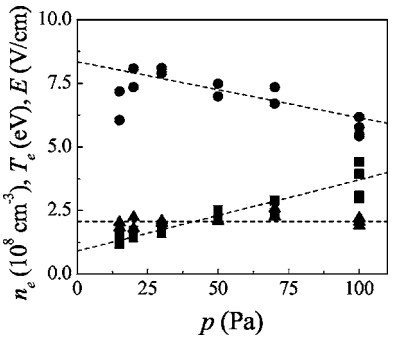

FIG. 2. Results of probe measurements [37]; electron temperature (circles), electron density (squares), and electric field (triangles). Dashed lines correspond to linear fits (see text).

temperature T_e [38]. The maximum of the first derivative of the probe current is used to estimate the plasma potential [38].

Results of the probe measurements of averaged values of n_e, T_e, and longitudinal electric field E, performed at the tube axis along with the linear fits used in the calculations below, are presented in Fig. 2. These linear fits are $n_e=(0.9+0.03p)\times 10^8$ cm^{-3}, $T_e=8.3-0.02p$ eV, and $E=2.1$ V/cm, where p is the pressure in Pascals. The axial values of plasma parameters are of interest for the analysis of experimental data because the particles form a cloud near central axis of the tube. The ion temperature is assumed to be close to the neutral gas (room) temperature, $T_i \simeq T_n \simeq 0.03$ eV, for the pressure range used.

B. Experimental procedure

We study the dynamics of particles of different size varying neutral gas pressure p and the number of injected particles N_d (controlled by settings of the particle dispenser), which allows us to change the particle number density n_d in the cloud. We then determine the grain charge by two different methods. (i) For a sufficiently low N_d the flow is stable for all pressures studied. The flow pattern is recorded for a number of different pressures. The charge can then be estimated from the *force balance* condition using the measured particle velocities. (ii) For larger N_d (and larger n_d) an easily identifiable transition to unstable flow (with a clear wave behavior) occurs at a certain threshold pressure p_*, which can be found experimentally with an accuracy of about 1 Pa [36,39]. A typical illustration of the transition to an unstable flow is shown in Fig. 3. This transition is a manifestation of the ion-dust streaming instability, caused by the relative drift between the particles and the ions. The value of p_* depends on n_d (shifting toward higher pressures when n_d is increased). The charge can be estimated from a *linear dispersion relation* describing the transition of the particle flow to the unstable regime at p_*. The force balance condition for pressures above p_* can also be used to estimate the charge. The detailed description of the theoretical models used in estimating the particle charge is given in Sec. III.

C. Effect of dust on discharge parameters

In order to estimate the particle charge from experimental observations, we have to know the plasma parameters. The

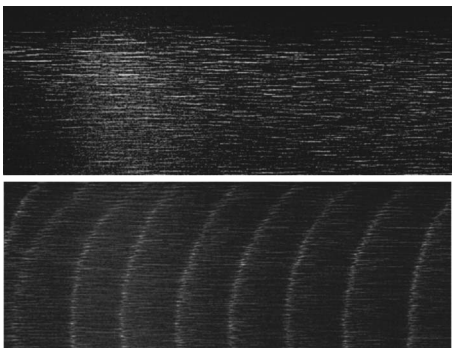

FIG. 3. Particle flow just above the threshold pressure at $p \simeq 56$ Pa (upper figure) and below it at $p \simeq 53$ Pa (lower figure) for the grains of radius $a \simeq 0.6$ μm. The grain number density $n_d=2.3\times 10^5$ cm^{-3}. Both pictures have a field of view of 6.4×4.8 mm^2. The center of the tube is located at the lower edge of the pictures.

latter are taken from the probe measurements performed in the absence of dust in the discharge. This requires that the effect of particles on discharge conditions is weak. Let us estimate when such an assumption is reasonable.

We adopt a simplified model for a positive column of a dc discharge without dust [40]. In this model the losses of electrons and ions to the walls of the tube (losses due to volume recombination are negligible in our case) are compensated by electron impact ionization. This requirement determines the electron temperature. The balance of the energy that electrons gain from the electric field and lose in the process of ionization and absorption on the walls (losses due to elastic electron-neutral collisions are small in our pressure range) yields a relation between the longitudinal electric field E and T_e. At a constant discharge current the average plasma density can be estimated from the electric field and electron mobility. Estimations of plasma parameters made with this simple model reproduce well the qualitative features of the probe measurements, i.e., weak decrease of T_e with p, almost constant electric field, and a linear increase of n_e with pressure. The quantitative difference between the estimated and measured values does not exceed a factor of 2.

The dust particles contribute to the momentum and energy exchange for electrons and ions and increase their losses. We use the ideas discussed in Refs. [41,42] to get a rough estimate of the conditions when the particle component starts to affect the discharge parameters significantly. This is expected to happen when the characteristic frequencies of the processes associated with the presence of particles become comparable to the frequencies of the same processes without the particles. We consider three processes: electron absorption on the particles, and momentum and energy exchange in electron-particle collisions. It can be shown that the characteristic frequencies of all three processes are practically the same (with the accuracy of a numerical coefficient of the order of unity),

$$\nu_e \sim \sqrt{8\pi} a^2 n_d v_{T_e}, \tag{1}$$

provided the condition $z \equiv Ze^2/aT_e \lesssim 1$ is satisfied. For simplicity we assume that the particles are distributed uniformly

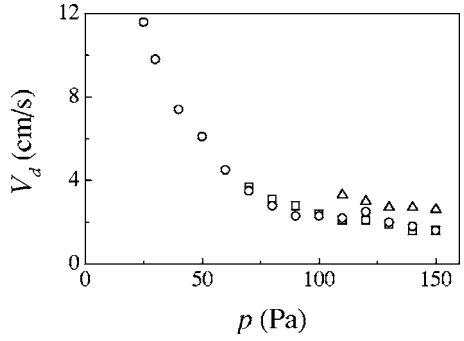

FIG. 4. Particle flow velocity V_d vs neutral gas pressure p for three values of particle number density. Circles correspond to $n_d \simeq 10^5$ cm^{-3}, squares to $n_d \simeq 4\times 10^5$ cm^{-3}, and triangles to $n_d > 4\times 10^5$ cm^{-3} (the image resolution does not permit more accurate estimate of n_d in this case.)

in the discharge tube. In this way we will overestimate the influence of dust, because in the experiments the radial extent of the particle cloud is always small compared to the tube radius.

The electron mobility is not affected if the momentum transfer frequency in electron-dust collisions is smaller than that in electron-neutral collisions. For the latter we have $\nu_{en} \simeq n_n \sigma_{en} v_{T_e}$, where n_n is the density of neutrals, $v_{T_e} = \sqrt{T_e/m_e}$ is the electron thermal velocity, and σ_{en} is the momentum transfer cross section for electron-neutral collisions, $\sigma_{en} \simeq 2\times 10^{-16}$ cm^2 in neon plasma with $T_e \gtrsim 1$ eV [43]. Using Eq. (1) the condition $\nu_e < \nu_{en}$ becomes $p/a^2 n_d \gtrsim 10^{-6}$, where p is in Pa, a is in μm, and n_d is in cm^{-3}. This inequality is always satisfied in our case. The losses of electrons and their energy in a dust-free discharge are characterized by a frequency $\nu_L \sim D_A/L^2$, where $D_A \simeq D_i(T_e/T_i)$ is the coefficient of ambipolar diffusion, $D_i \simeq v_{T_i}^2/\nu_{in}$ is the diffusion coefficient of ions, $\nu_{in} = n_n \sigma_{in} v_{T_i}$ is the momentum transfer frequency in ion-neutral collisions, and $L \simeq 2.4R$ [40]. The condition $\nu_e < \nu_L$ with the help of Eq. (1) yields the inequality $pa^2 n_d \lesssim (1.1 T_e v_{T_i}/\sigma_{in} R^2 v_{T_e})$, under which the presence of dust does not affect loss of electrons and their energy. Inserting $T_e \sim 7$ eV, $\sigma_{in} \sim 10^{-14}$ cm^{-2}, $R = 1.5$ cm we get $pa^2 n_d \lesssim 1.5\times 10^6$, where again p is in Pa, a is in μm, and n_d is in cm^{-3}.

We see from these estimates that the effect of the dust component can be important for sufficiently large particle column density $a^2 n_d$—a result which is intuitively expected. This mainly limits the applicability of the linear dispersion relation method because higher particle densities are required to produce unstable flows at higher pressures. In practice we used this method for smaller grains only, at particle density below $n_d \simeq 4\times 10^5$ cm^{-3} (corresponding to p_* of approximately 60 Pa). Although these numbers give us an acceptable pressure range $0.1 \lesssim p \lesssim 10$ Pa, we recall that our consideration overestimates the influence of dust. An experimental confirmation that the plasma parameters are not strongly modified by the presence of particles can be derived from the observation that the flow velocity is insensitive to $N_d(n_d)$. This is illustrated in Fig. 4, which shows the measured particle velocity as a function of pressure for particles of radius $a \simeq 0.6$ μm and three different values of n_d. We see that the difference in the velocities is insignificant as long as $n_d \lesssim 4\times 10^5$ cm^{-3}. For larger particles we observed that the flow velocity starts to increase with N_d at lower particle densities. We attribute this to non-negligible effect of dust on plasma parameters. Consequently, we do not use the linear dispersion relation method for large particles. For the force balance method the settings of the dispenser were adjusted to provide the lowest possible value of $n_d \sim 10^4$–10^5 cm^{-3} in order to minimize the effect of dust on discharge parameters.

The presence of the particles affects the charge composition of the complex plasma cloud through the quasineutrality requirement, $n_e + Zn_d = n_i$. When the particles do not contribute to the balance conditions for the electrons, the average value of n_e is unaffected by the presence of particles at a constant discharge current $I \propto n_e u_e$ (where u_e is the electron drift velocity), because neither the electron mobility nor T_e and E is modified. In this case we expect n_i to somewhat increase to ensure charge neutrality.

III. THEORETICAL MODELS

Below we present the theoretical basis for the two methods used for charge estimation.

A. Force balance method

The velocity of particles in a stable flow is determined by the balance of the forces acting on them: The electric force $F_{el} = -ZeE$, the neutral drag force $F_n = -m_d \nu_{dn} V_d$, the ion drag force $F_i = m_d \nu_{di}(u_i - V_d) \simeq m_d \nu_{di} u_i$, and the electron drag force $F_e = m_d \nu_{de}(u_e - V_d) \simeq m_d \nu_{de} u_e$. Here m_d is the dust particle mass, $u_i(u_e)$ is the ion (electron) drift velocity, and ν_{dn}, ν_{di}, and ν_{de} are the effective momentum transfer frequencies in dust-neutral, dust-ion, and dust-electron collisions, respectively. For our conditions the electron drag force is almost two orders of magnitude smaller than the ion drag force due to the large value of electron-to-ion temperature ratio $\tau = T_e/T_i$ (see Ref. [44] for details). Thus, the force balance is given by

$$F_{el} + F_i + F_n \simeq 0. \tag{2}$$

For the momentum transfer in dust-ion collisions we use

$$m_d \nu_{di} = (8\sqrt{2\pi}/3) a^2 n_i m_i v_{T_i} \left(1 + \frac{\beta_T}{2}\frac{\lambda}{a} + \frac{\beta_T^2}{4}\frac{\lambda^2}{a^2}\Lambda\right), \tag{3}$$

where m_i is the ion mass, $v_{T_i} = \sqrt{T_i/m_i}$ is the ion thermal velocity, and $\Lambda = 2\int_0^\infty \exp(-x)\ln[(2x+\beta_T)/(2ax/\lambda + \beta_T)]dx$ is the *modified* Coulomb logarithm integrated over the Maxwellian velocity distribution function for ions [45]. We have introduced the *thermal scattering parameter* $\beta_T = Ze^2/T_i\lambda$, which is essentially the ratio of the Coulomb radius for ion-particle interaction, $R_C = Ze^2/T_i$, to the plasma screening length λ [45–47]. This parameter characterizes ion coupling to the particle: coupling is weak when $\beta_T \ll 1 (R_C \ll \lambda)$ and is strong in the opposite limit. In deriving Eq. (3) Yukawa potential for ion-grain interaction is accepted and a subthermal ion drift ($u_i \lesssim v_{T_i}$) is assumed, which also implies that the

effective screening length is close to the ion Debye radius, $\lambda \simeq \lambda_{Di} = \sqrt{T_i/4\pi e^2 n_i}$ [48,49]. Expression (3) is applicable for weak and moderate coupling between the particle and the ions, $\beta_T \lesssim 5$ [45–47], which is the case for the relatively small grains and plasma conditions investigated. In addition, it is derived for collisionless ions: ion mean free path should be large compared to the characteristic length scale of ion-grain interaction ($\sim R_C$ for $\beta \ll 1$ and $\sim\lambda$ for $\beta \sim 1$). This condition is not always satisfied in our experiment so we also considered the model of Ref. [50] developed for the ion drag force in a *collisional* plasma in the regime of weak ion-grain coupling ($\beta \ll 1$), which predicts an enhancement in the force at $\ell_i \ll \lambda$. However, under the conditions investigated this model yields the ion drag force which is considerably smaller than that from Eq. (3). Thus, the effect of moderate ion-grain coupling is apparently more important in the present experiment. In addition, for "high" pressures ($p \gtrsim 50$ Pa) the ion drag force, calculated with the use of Eq. (3), is a small fraction of the electric force and some inaccuracy introduced by neglecting collisions should not significantly affect the charge estimation in this case.

The ion drift velocity is determined by ion-neutral and ion-dust collisions, $u_i \simeq eE/m_i \nu_i^{\text{eff}}$, where $\nu_i^{\text{eff}} = \nu_{in} + \nu_{id}$, where $\nu_{id} = \nu_{di}(m_d n_d / m_i n_i)$ is the momentum loss frequency of the ions in ion-dust collisions. For ν_{in} we use $\nu_{in} = n_n \sigma_{in} v_{T_i}$, with a *constant* effective momentum transfer cross section which takes into account both charge exchange and polarization interaction, $\sigma_{in} \simeq 10^{-14}$ cm^2 [51,52]. For most of the complex plasma conditions investigated here ν_{in} is considerably larger than ν_{id}.

For the momentum transfer in dust-neutral collisions we have $m_d \nu_{dn} = (8\sqrt{2\pi}/3)\delta a^2 n_n m_n v_{T_n}$, where m_n and v_{T_n} are the mass and thermal velocity of neutrals, respectively [53]. The numerical factor $\delta = 1 + \pi/8 \simeq 1.4$, corresponding to diffuse scattering with full accommodation is consistent with recent experimental results [54].

B. Linear dispersion relation method

Though linear theory might not be applicable to describe the nonlinear wave modes observed in the experiment, it should be adequate to predict the onset of self-excited waves at p_*. The dispersion relation can be written in the form

$$1 + \chi_e + \chi_i + \chi_d = 0, \tag{4}$$

where χ_e, χ_i, and χ_d are the susceptibilities of the electron, ion, and dust components, respectively. In deriving a dispersion relation for very low frequency waves associated with the dust dynamics we use static susceptibilities of electrons and ions. Assumption of the Boltzmann response for the electrons yields

$$\chi_e = (k\lambda_{De})^{-2}, \tag{5}$$

where k is the wave number and $\lambda_{De} = \sqrt{T_e/4\pi e^2 n_e}$ is the electron Debye radius. The effect of the electron drift in the discharge electric field can be also incorporated (see, e.g., [36]), but it is negligible in our case. The static susceptibility of the ion component within the hydrodynamic approach, taking into account ion drift and collisions, can be written as [55–58]

$$\chi_i = \frac{\omega_{pi}^2}{k^2 v_{T_i}^2 + k u_i (i\nu_i^{\text{eff}} - k u_i)}, \tag{6}$$

where $\omega_{pi} = v_{T_i}/\lambda_{Di}$ is the ion plasma frequency. The same result can be obtained for collisional ($\nu_i^{\text{eff}} \gg k v_{T_i}$) Maxwellian ions within a kinetic approach using the model Bhattnagar-Gross-Krook collision integral (see e.g., [59]). We note that for the range of threshold pressures studied the ion drift is subthermal, $u_i < v_{T_i}$. This implies that the deviation of the ion velocity distribution function from the shifted Maxwellian, which can be quite significant for $u_i \gtrsim v_{T_i}$ [60–62], is small. The susceptibility of the drifting "cold" ($V_d \gg v_{Td}$) dust component is

$$\chi_d = -\frac{\omega_{pd}^2}{(\omega + kV_d)(\omega + kV_d + i\nu_{dn})}, \tag{7}$$

where ω is the wave frequency and $\omega_{pd} = \sqrt{4\pi Z^2 e^2 n_d / m_d}$ is the dust plasma frequency. Equations (4)–(7) identify the dispersion relation used in this work. [Note that there is a misprint in Ref. [36] in the dust grain susceptibility (χ_d), where ω appeared instead of $\omega + kV_d$.]

C. Numerical solution

We solve Eqs. (2) and (4) numerically using the plasma parameters taken from the probe measurements and the quasineutrality condition. Thus, in our calculations n_i, ν_{di}, ν_{id}, u_i, ω_{pi}, and ω_{pd} are functions of the particle charge only. Equation (2) is solved directly, yielding the particle charge. Solution of the dispersion relation (4) gives the dependence of $\omega = \omega_r + i\omega_i$ on the wave number k for a given particle charge. The charge is then determined by matching the experimental observations: Stable mode ($\omega_i < 0$ for all k) above the threshold pressure p_* and unstable mode ($\omega_i > 0$ for a range of k, corresponding to experimentally found wavelengths) below p_*. An illustration of such a solution is shown in Fig. 5.

IV. MOLECULAR DYNAMICS SIMULATIONS

To have an independent verification of the charge estimates described above, molecular dynamics (MD) simulations of particle charging have been carried out for conditions similar to the experiment. The simulations are performed using a code originally developed by Zobnin *et al.* [22] to study the effect of ion-neutral collisions on the charging of an individual particle in a quasineutral plasma. The following modifications are made to the code to take into account the effect of finite particle density. A grain is placed in a spherical cell with the radius equal to the Wigner-Seitz radius $\left(\frac{4\pi}{3} n_d\right)^{-1/3}$. The number of the ions inside the cell is chosen so that the "global" electron number density corresponds to the value found from probe measurements. Electrons obey the Boltzmann distribution inside the cell. The equations of motion for the ions are solved including for ion-neutral charge-exchange collisions and ion absorption on

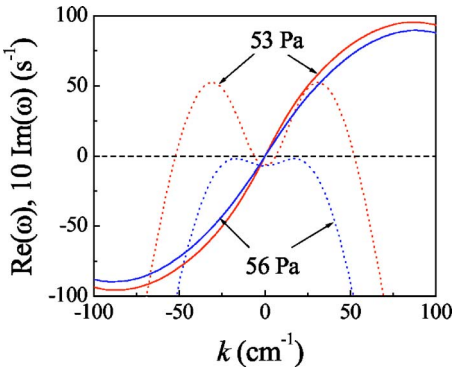

FIG. 5. (Color online) Numerical solution of the linear dispersion relation (4). The dust number density and threshold pressure correspond to those of Fig. 3. Real and imaginary parts of ω are given by solid and dashed lines, respectively (note that the imaginary parts are multiplied by a factor 10). Upper (lower) lines correspond to $p=53$ (56) Pa. Particle charge number in this calculation is $Z=2\times10^3$.

the particle surface (with sticking coefficient equal to unity); the outer boundary condition is specular reflection. Finally, the loss of the ions absorbed on the particle surface is compensated by creation of new ions. These new ions have a Maxwellian velocity distribution corresponding to the neutral gas temperature. The probability to be created in a certain region within the cell is proportional to the local electron number density.

The charges obtained using this modified code are smaller than those obtained with the original code. This is caused by an increase in the ion density compared to the electron density (effect of closely packed grains). However, the difference is not very significant (usually less than 10%) for the conditions investigated. For this reason we use only the results of MD simulations obtained for an individual particle.

V. ANALYTICAL APPROXIMATION FOR GRAIN CHARGING

In this section we present a simple analytical approximation which takes into account the effect of (rare) ion-neutral collisions on the particle charging.

Schulz and Brown [63] and Zakrzewski and Kopiczinski [25] made the following argument for the role of ion neutral collisions in the perturbed plasma region ("sheath" in their notation) around a probe. They noted that the collisions in the sheath cause the destruction of the ion orbital motion. When an orbiting ion makes a collision in the sheath it will lose energy and be trapped in the region of high negative potential. Such an ion cannot escape and will eventually reach the probe surface. Especially effective are charge-exchange collisions which lead to a substitution of the original ion by a low energy ion "created" from neutrals. In this case essentially every charge-exchange collision in the sheath will result in an ion absorption on the probe surface, either directly or through subsequent collisions. Thus, when an average ion experiences not too many collisions in the perturbed plasma region, the collisions lead to an increase in the ion flux to the probe. On the other hand, when the gas pressure is so high that ions make many collisions on their way to the probe, then their motion is controlled by mobility. Mobility decreases with pressure and so does the ion flow. These arguments are used to explain a maximum in the ion current collected by a negatively biased probe occurring with increasing neutral gas pressure [25,27,28].

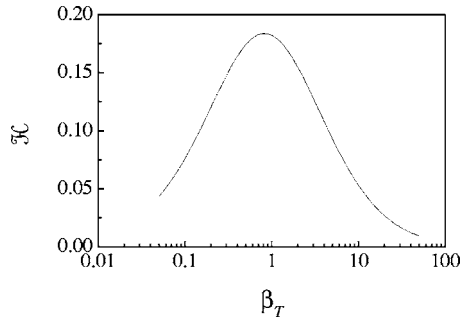

FIG. 6. Dependence of the function $\mathcal{H}$ on the thermal scattering parameter β_T (for details see text).

To obtain an approximation for the ion current to the particle in the presence of ion-neutral collisions we use the ideas discussed by Zakrzewski and Kopiczinski [25] and more recently by Zobnin *et al.* [22] and Lampe *et al.* [24]. First let us define a relevant (for this particular problem) length scale for the perturbed plasma region, R_0. Since the energy of an ion after charge-exchange collision is $\sim T_n \sim T_i$ it is convenient to assume that R_0 can be determined from the condition $|U(R_0)| \simeq T_i$, where $U(r)$ denotes the potential energy of ion-grain interaction. For the Yukawa potential the radius of the perturbed region normalized to the plasma screening length, R_0/λ, is given by the root of the transcendental equation $\beta_T \exp(-x)=x$, where $\beta_T=z\tau(a/\lambda)$. For weak ion-grain coupling ($\beta_T \ll 1$) we have $R_0 \approx R_C$, while for moderate coupling ($\beta_T \sim 1$) we have $R_0 \sim \lambda$.

We consider here the *weakly collisional regime* for the ions, characterized by the condition $\ell_i \gtrsim R_0$. Beyond the sphere of radius R_0 the plasma density is weakly perturbed, ions have Maxwellian velocity distribution and their random flux into the perturbed region is given by $I_{R_0} \simeq \sqrt{8\pi} R_0^2 n_i v_{T_i}$. The probability for an ion to experience charge-exchange collision inside the perturbed region can be roughly estimated as $\sim R_0/\ell_i$, provided $R_0/\ell_i < 1$. As discussed above the ion after the collision is very likely absorbed on the particle. Thus, the net ion flux on the particle is simply given by the sum of the OML flux $I_{\mathrm{OML}}=\sqrt{8\pi}a^2 n_i v_{T_i}(1+z\tau)$ and the "collisional" contribution $(I_{R_0}-I_{\mathrm{OML}})(R_0/\ell_i)$. This leads to the expression derived by Lampe *et al.* [24]

$$I_i \simeq \sqrt{8\pi} a^2 n_i v_{T_i} [1 + z\tau + (R_0^3/a^2\ell_i)]. \tag{8}$$

In view of the numerous approximations made in deriving expression (8) it is convenient to further simplify it. We note that the last term in the parentheses in Eq. (8) can be rewritten in the form $\mathcal{H}(\beta_T) z^2 \tau^2 (\lambda/\ell_i)$, where $\mathcal{H}(\beta_T)=(R_0/\lambda)^3 \beta_T^{-2}$. The dependence $\mathcal{H}(\beta_T)$ is plotted in Fig. 6. The function $\mathcal{H}$ has the following asymptotes: For $\beta_T \ll 1$ we have $\mathcal{H} \sim \beta_T$, while for $\beta_T \gg 1$ we have $\mathcal{H} \sim \beta_T^{-2} \ln^3 \beta_T$. In the parameter

regime $0.1 \lesssim \beta_T \lesssim 10$, typical for laboratory complex plasmas, $\mathcal{H}$ is a relatively weak function of β_T with the characteristic value $\mathcal{H} \sim 0.1$. Neglecting also unity compared to a large factor $z\tau$ we get

$$I_i \simeq \sqrt{8\pi} a^2 n_i v_{T_i} z\tau [1 + 0.1 z\tau(\lambda/\ell_i)], \quad (9)$$

From Eq. (9) we can see that the contribution to charging flux due to ion-neutral collisions is dominant when $\ell_i \lesssim 0.1 z\tau\lambda$. For typical dusty plasma parameters $z \sim 1$ and $\tau \sim 100$ collisions affect particle charging even when the mean free path is an order of magnitude larger than the screening length.

To calculate the particle charge it is necessary to equate the ion flux to the electron flux, $I_e = \sqrt{8\pi} a^2 n_e v_{T_e} \exp(-z)$. If Eq. (9) is used for the ion flux, then z depends on τ and λ/ℓ_i, but is independent of the ratio a/λ. There is a case when the approximate expression for z is particularly simple; namely, assuming $0.1 z\tau(\lambda/\ell_i) \gg 1$ and $z \lesssim 1$ we get from the flux balance $z \sim (3/\tau)(v_{T_e}/v_{T_i})^{1/2}(\ell_i/\lambda)^{1/2}$, which can be used for rough estimations of particle charge in laboratory experiments.

VI. RESULTS AND DISCUSSION

The experimental results for three different particle sizes are presented in Fig. 7. For the smallest particles both experimental methods demonstrate good agreement. For two larger particles only the force balance method is used. The error bars correspond to the uncertainties in n_d (50%), n_e (30%), E (10%), and V_d (15%). Both methods are quite insensitive to the value of T_e. As seen from Fig. 7 the charges found from MD simulations agree well with the experimental results. Some discrepancies can be attributed to the simplifications made in estimating the charge from experiments.

Figure 7 also shows the results of calculations using different theoretical models. Dotted lines correspond to a modification of the collisionless OML theory, which takes into account the effect of a finite particle number density, i.e., the dust contribution to the quasineutrality condition. In the simplest approximation the charging equation is $v_{T_e} \exp(-z) = v_{T_i}(1 + z\tau)(1 + P)$ [12]. Two lines in each figure correspond to the maximum (lower line) and minimum (upper line) values of the Havnes parameter P, which are estimated from experimentally determined charges and particle densities. We see from Fig. 7 that even with the finite particle density taken into account the collisionless OML theory overestimates considerably the charge compared to the results of experiments and MD simulations. It is important to note that the largest values of P occur at low pressures due to low plasma density and high particle charge. For "high" pressures ($p \gtrsim 50$ Pa) the Havnes parameter is considerably smaller than unity, and, in addition, $\Delta/\lambda \gg 1$. This implies that quasineutrality is weakly affected by the particle component, and so are electron and ion trajectories by neighboring grains. This leads us to the conclusion that the effect of closely packed grains is insignificant in this pressure range. Our experiment was performed in the regime of moderate ion-grain coupling

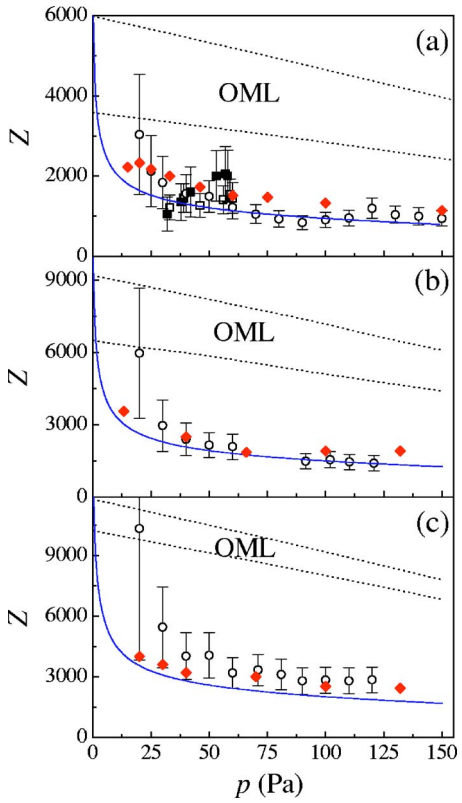

FIG. 7. (Color online) Particle charge number Z as a function of neutral gas pressure p for three different particle radii: $a \simeq 0.6$ (a), $\simeq 1.0$ (b), and $\simeq 1.3$ μm (c). Symbols correspond to the particle charge obtained from experiments [force balance for low number of injected particles (open circles); force balance for pressures above the threshold (open squares), solution of dispersion relation (solid squares)] and from MD simulations for individual particles (solid diamonds). The areas between two dotted lines in each figure correspond to the charge given by the collisionless OML model modified to take into account a finite particle density for the Havnes parameters (calculated from experimental data) in the ranges $0.2 < P < 3$ (a), $0.3 < P < 2$ (b), and $0.4 < P < 1$ (c). Solid lines show calculations using an analytical approximation of Eq. (8) for the ion flux to the particle in a weakly collisional regime for the ions.

($\beta_T \lesssim 5$ for largest particles) and hence the effect of the barrier in the effective potential energy can be neglected as well [20]. Therefore, the dramatic charge suppression (up to 3–4 times) at high pressures is attributed mainly to the effect of ion-neutral collisions.

Solid lines in Fig. 7 correspond to a simple analytical approximation for the particle charge in the weakly collisional regime for the ions. They are calculated using expression (8) for the ion flux and assuming an individual particle ($n_i \sim n_e$). The dependence of plasma parameters on the neutral gas pressure is taken from the probe measurements. Figure 7 demonstrates good agreement of these calculations with the results of experiments and MD simulation. Hence, the simple analytical approximation provides not only a correct qualitative picture of the effect of ion-neutral collisions on particle charging but also can be used for quantitative estimations. We point out here that the experimental data for lowest pressures, for which the deviation from the analytical

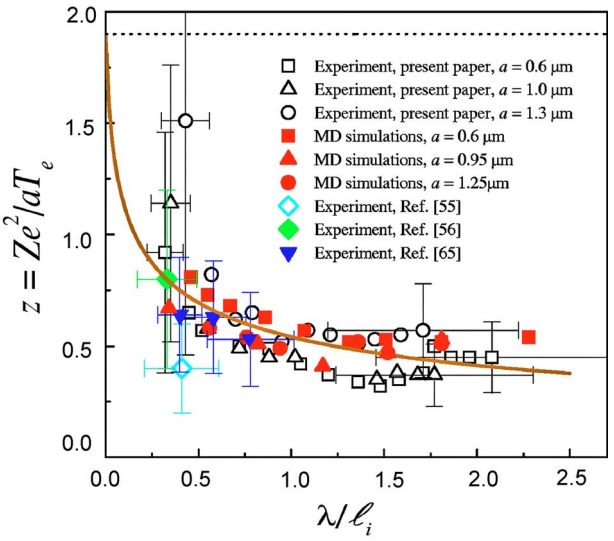

FIG. 8. (Color online) The dimensionless particle charge $z = Ze^2/aT_e$ as a function of the ion collisionality parameter, λ/ℓ_i. Open symbols correspond to the particle charges measured in the present experiment from the force balance condition for $a \simeq 0.6$ (squares), $\simeq 1.0$ (triangles), and $\simeq 1.3$ μm (circles). For clarity error bars are shown only for minimal and maximal values of λ/ℓ_i. Solid squares, triangles, and circles are the charges from MD simulation for $a = 0.6$, 0.95, and 1.25 μm, respectively. Open (solid) diamond corresponds to the experimental results reported in Ref. [55] (Ref. [56]). Solid down triangles correspond to the charges obtained in Ref. [65]. The dotted line is calculated using the collisionless OML approach for an individual particle. The solid line shows a calculation using an analytical approximation of Eq. (9) for the ion flux to the particle in the weakly collisional regime for the ions. In these analytical calculations we assume $T_e = 7$ eV.

results and numerical simulations is relatively large, may contain significant systematic errors as discussed in Sec. VII.

Let us compare the obtained results with other available experimental results on particle charges in the bulk plasmas of gas discharges.

The first two experiments we take for comparison were performed under microgravity conditions with the use of the PKE-Nefedov facility operating onboard the ISS [64]. They employ a symmetrically driven parallel plate capacitively coupled rf discharge. The particles injected in the discharge form a cloud between the electrodes. It is possible to excite the waves in the particle cloud by applying a low frequency modulation voltage to the electrodes. The charge can then be estimated by comparing the measured dispersion relations with the theoretical ones. In this way the dimensionless charge was found to be $z \sim 0.4$ (at $p \simeq 25$ Pa argon gas pressure) [55] and $z \sim 0.8$ (at $p \simeq 12$ Pa argon gas pressure) [56]. The results of these experiments are shown in Fig. 8 by open and solid diamond, respectively. The errors were not estimated, but it is rather unreasonable to expect an accuracy better than $\sim 50\%$ in both z and λ/ℓ_i due to uncertainties in plasma parameters and approximations made in deriving theoretical dispersion relations.

Another experimental method to determine the particle charge reported recently is based on gravity-driven heavy "test" particle collisions with smaller particles levitating in the quasiisotropic region of an inductively coupled rf discharge plasma [65]. A heavy particle falls down in a vertical glass tube and interacts with the cloud of small particles suspended in the diffuse edge of the discharge. The interaction process is recorded with a high-speed video camera and individual elastic collisions are analyzed. Assuming the Yukawa potential around each particle both the particle charge and effective screening length can be estimated. In Ref. [65] the particle charge was estimated for three different pressures of neon gas (20, 30, and 50 Pa). The results are shown in Fig. 8 by solid downward pointing triangles. Error bars correspond to $\sim 40\%$ uncertainty in z (due to $\sim 30\%$ uncertainty in Z and T_e), and $\sim 30\%$ uncertainty in λ/ℓ_i.

In Fig. 8 we combine available experimental, analytical, and numerical results in a $(z, \lambda/\ell_i)$ diagram, where λ/ℓ_i is the ion "collisionality parameter (index)" [24]. The figure demonstrates reasonable agreement between the results of different experiments, although they were performed under completely different plasma conditions (e.g., different types of discharges, different gases, different particle sizes, and different plasma parameters). This indicates that the collisionality index λ/ℓ_i is one of the most important parameters, which controls the particle charge in isotropic dusty plasmas. The results of numerical simulations are in good agreement with the experimental results. The obtained charges are much smaller than the collisionless OML theory predicts (dotted line). At the same time a simple analytical approximation of Eq. (9) provides a reasonable fit for the available experimental and numerical data (solid line). (To simplify calculations we assumed a constant value of the electron temperature $T_e = 7$ eV, so that $\tau \simeq 233$ and $\sqrt{v_{T_e}/v_{T_i}} \simeq 50$.) In the parameter regime investigated $R_0/\ell_i \lesssim 1$ and the dimensionless charge decreases with the ion collisionality parameter, in agreement with Eq. (9). Note, however, that for sufficiently large ion collisionality ($R_0/\ell_i \gtrsim 1$) the assumptions used in deriving Eq. (9) are no longer satisfied. At $R_0/\ell_i \gg 1$ a transition to mobility-limited (hydrodynamic) regime of ion collection should occur. In this regime the charge increases with collisionality (see, e.g., Refs. [22,66]). This regime is, however, outside of the pressure range studied.

VII. CRITICAL ASSESSMENT OF THE SIMPLIFYING ASSUMPTIONS

Several simplification were implicitly used when estimating the particle charge in our experiment. Let us consider their possible effect on the accuracy of the obtained results.

For the analysis we used the values for plasma parameters measured at the tube axis. In fact, it was observed that the particle cloud was shifted systematically downward with increasing particle size. This is because stronger electric fields were required to levitate larger particles. Thus the plasma parameters could be different in regions of levitation for different particles. However, the radial electric field required to levitate the largest particles ($a \simeq 1.3$ μm) was still relatively weak, $E_\perp \simeq (m_d g/Ze) \sim 2$ V/cm, i.e., $E_\perp \lesssim E$. The ion drift is subthermal for these conditions, i.e., plasma is quasiisotropic. For this reason we do not expect significant differences

in plasma parameters for different particles in our experiment.

We assumed subthermal ion drift and constant momentum transfer cross section for ion-neutral collisions. These approximations break down at $u_i/v_{T_i} \simeq eE\ell_i/T_i \simeq 1$, which yields $p \sim 30$ Pa. Experimental results for lower pressures can contain some systematic errors.

The force balance method is sensitive to the ion drag force model employed, especially for low pressures, when F_i and F_{el} are comparable. Here the inaccuracy of the model (associated, for example, with the assumption $u_i \lesssim v_{T_i}$) can contribute to systematic errors. However, for "high" pressures, $p \gtrsim 50$ Pa, we have $|F_i/F_{\mathrm{el}}| \lesssim 0.3$ and hence the results are not very sensitive to the ion drag force model.

In spite of the estimates made in Sec. II C we cannot completely exclude the possibility of some modification of discharge parameters due to the presence of particles. This effect can be particularly important for large n_d and P, which correspond to low pressures or to the results obtained with the linear dispersion relation method.

Summarizing, the largest errors, both random and systematic, are expected for lowest pressures investigated. At high pressures, where the deviation from the collisionless OML theory is most pronounced, the experimental results are reliable. In this regime the effects of closely packed grains and the barrier in the effective potential energy for the ions are not important. Hence, charge reduction is mainly associated with ion-neutral collisions, the conclusion supported by MD simulations and analytical approximation.

VIII. CONCLUSIONS

We have determined the charge of dust particles in a bulk dc discharge plasma under conditions when the ion mean free path is comparable to the plasma screening length. Two independent experimental methods and MD simulations agree well with one another and yield a charge which is significantly smaller than that predicted by collisionless orbital motion limited theory. Other available measurements of the particle charge in the bulk of gas discharges are in reasonable agreement with the results of our present experiment. The main process affecting and regulating the particle charge is identified: ion-neutral collisions. A simple analytical approximation is shown to be appropriate to estimate the particle charge in the weakly collisional regime for the ions.

ACKNOWLEDGMENTS

The authors would like to thank K. Tarantik and Yu. Gerasimov for skillful technical assistance. This work was supported by DLR under Contract No. 50 WP 0204.

[1] C. K. Goertz, Rev. Geophys. **27**, 271 (1989).
[2] P. Bliokh, V. Sinitsin, and V. Yaroshenko, *Dusty and Self-Gravitational Plasmas in Space* (Kluwer, Dordrecht, 1995).
[3] E. C. Whipple, Rep. Prog. Phys. **44**, 1197 (1981).
[4] L. Boufendi and A. Bouchoule, Plasma Sources Sci. Technol. **11**, A211 (2002).
[5] H. Kersten *et al.*, Contrib. Plasma Phys. **41**, 598 (2001).
[6] V. N. Tsytovich and J. Winter, Phys. Usp. **41**, 815 (1998).
[7] J. Winter, Phys. Plasmas **7**, 3862 (2000).
[8] H. M. Thomas and G. E. Morfill, Nature (London) **379**, 806 (1996).
[9] G. E. Morfill *et al.*, Phys. Scr., T **107**, 59 (2004).
[10] G. E. Morfill *et al.*, Contrib. Plasma Phys. **44**, 450 (2004).
[11] G. E. Morfill *et al.*, Phys. Rev. Lett. **92**, 175004 (2004).
[12] V. E. Fortov, A. G. Khrapak, S. A. Khrapak, V. I. Molotkov, and O. F. Petrov, Phys. Usp. **47**, 447 (2004).
[13] J. E. Allen, Phys. Scr. **45**, 497 (1992).
[14] R. V. Kennedy and J. E. Allen, J. Plasma Phys. **69**, 485 (2003).
[15] O. Havnes, G. E. Morfill, and C. K. Geortz, J. Geophys. Res. **89**, 10999 (1984).
[16] A. Barkan, N. D'Angelo, and R. L. Merlino, Phys. Rev. Lett. **73**, 3093 (1994).
[17] Ya. L. Al'pert, A. V. Gurevich, and L. P. Pitaevskii, *Space Physics with Artificial Satelites* (Plenum Press, New York, 1995).
[18] J. E. Allen, B. M. Annaratone, and U. de Angelis, J. Plasma Phys. **63**, 299 (2000).
[19] M. Lampe, J. Plasma Phys. **65**, 171 (2001).
[20] S. A. Khrapak, A. V. Ivlev, and G. E. Morfill, Phys. Rev. E **70**, 056405 (2004).
[21] J. Goree, Plasma Sources Sci. Technol. **3**, 400 (1994).
[22] A. V. Zobnin, A. P. Nefedov, V. A. Sinel'shchikov, and V. E. Fortov, JETP **91**, 483 (2000).
[23] M. Lampe, V. Gavrishchaka, G. Ganguli, and G. Joyce, Phys. Rev. Lett. **86**, 5278 (2001).
[24] M. Lampe *et al.*, Phys. Plasmas **10**, 1500 (2003).
[25] Z. Zakrzewski and T. Kopiczynski, Plasma Phys. **16**, 1195 (1974).
[26] Z. Sternovsky and S. Robertson, Appl. Phys. Lett. **81**, 1961 (2002).
[27] Z. Sternovsky, S. Robertson, and M. Lampe, J. Appl. Phys. **94**, 1374 (2003).
[28] F. Taccogna, S. Longo, and M. Capitelli, Contrib. Plasma Phys. **44**, 594 (2004).
[29] A. Melzer, A. Trottenberg, and A. Piel, Phys. Lett. A **191**, 301 (1994).
[30] A. Homann, A. Melzer, and A. Piel, Phys. Rev. E **59**, R3835 (1999).
[31] E. B. Tomme, D. A. Law, B. M. Annaratone, and J. E. Allen, Phys. Rev. Lett. **85**, 2518 (2000).
[32] V. E. Fortov, A. P. Nefedov, V. I. Molotkov, M. Y. Poustylnik, and V. M. Torchinsky, Phys. Rev. Lett. **87**, 205002 (2001).
[33] A. Piel and A. Melzer, Plasma Phys. Controlled Fusion **44**, R1 (2002).
[34] A. A. Samarian and S. V. Vladimirov, Phys. Rev. E **67**, 066404 (2003).
[35] C. M. Ticos, A. Dyson, and P. W. Smith, Plasma Sources Sci.

Technol. **13**, 395 (2004).
[36] S. Ratynskaia *et al.*, Phys. Rev. Lett. **93**, 085001 (2004).
[37] A. Usachev *et al.*, Czech. J. Phys. **54**, C639 (2004).
[38] V. Demidov, S. Ratynskaia, and K. Rypdal, Rev. Sci. Instrum. **73**, 3409 (2002).
[39] S. Ratynskaia *et al.*, IEEE Trans. Plasma Sci. **32**, 613 (2004).
[40] Yu. P. Raizer. *Gas Discharge Physics* (Springer, Berlin, 1991).
[41] J. P. Boeuf, Phys. Rev. A **46**, 7910 (1992).
[42] A. M. Lipaev *et al.*, JETP **85**, 1110 (1997).
[43] A. Gilardini, *Low Energy Electron Collisions in Gases* (Wiley, New York, 1972).
[44] S. A. Khrapak and G. E. Morfill, Phys. Rev. E **69**, 066411 (2004).
[45] S. A. Khrapak, A. V. Ivlev, G. E. Morfill, and H. M. Thomas, Phys. Rev. E **66**, 046414 (2002).
[46] S. A. Khrapak, A. V. Ivlev, G. E. Morfill, and S. K. Zhdanov, Phys. Rev. Lett. **90**, 225002 (2003).
[47] S. A. Khrapak, A. V. Ivlev, G. E. Morfill, S. K. Zhdanov, and H. M. Thomas, IEEE Trans. Plasma Sci. **32**, 555 (2004).
[48] S. A. Khrapak *et al.*, Phys. Plasmas **10**, 4579 (2003).
[49] S. A. Khrapak, A. V. Ivlev, S. K. Zhdanov, and G. E. Morfill, Phys. Plasmas **12**, 042308 (2005).
[50] A. V. Ivlev, S. A. Khrapak, S. K. Zhdanov, G. E. Morfill, and G. Joyce, Phys. Rev. Lett. **92**, 205007 (2004).
[51] M. A. Biondi and L. M. Chanin, Phys. Rev. **94**, 910 (1954).
[52] R. N. Varney, Phys. Rev. **88**, 362 (1952).
[53] P. S. Epstein, Phys. Rev. **23**, 710 (1921).
[54] B. Liu, J. Goree, V. Nosenko, and L. Boufendi, Phys. Plasmas **10**, 9 (2003).
[55] S. Khrapak *et al.*, Phys. Plasmas **10**, 1 (2003).
[56] V. V. Yaroshenko *et al.*, Phys. Rev. E **69**, 066401 (2004).
[57] S. A. Khrapak and V. V. Yaroshenko, Phys. Plasmas **10**, 4616 (2003).
[58] G. Joyce, M. Lampe, and G. Ganguli, Phys. Rev. Lett. **88**, 095006 (2002).
[59] A. F. Alexandrov, L. S. Bogdankevich, and A. A. Rukhadze, *Principles of Plasma Electrodynamics* (Springer, New York, 1984).
[60] V. A. Schweigert, Plasma Phys. Rep. **27**, 997 (2001).
[61] A. V. Ivlev, S. K. Zhdanov, S. A. Khrapak, and G. E. Morfill, Plasma Phys. Controlled Fusion **46**, B267 (2004).
[62] A. V. Ivlev, S. K. Zhdanov, S. A. Khrapak, and G. E. Morfill, Phys. Rev. E **71**, 016405 (2005).
[63] G. J. Schulz and S. C. Brown, Phys. Rev. **98**, 1642 (1955).
[64] A. Nefedov *et al.*, New J. Phys. **5**, 33 (2003).
[65] V. E. Fortov, O. F. Petrov, A. D. Usachev, and A. V. Zobnin, Phys. Rev. E **70**, 046415 (2004).
[66] P. Bryant, J. Phys. D **36**, 2859 (2003).